Particle Orbit Correction in an Energy Recovery Linac

Changsheng Song, Georg Hoffstaetter
Laboratory of Elementary Particle Physics, Cornell University

July 31, 2007

Abstract

In this report, we first consider four common sources of closed orbit errors that can occur in a linear accelerator: quadrupole misalignment errors, quadrupole magnetic field errors, dipole magnetic field errors and RF cavity pitch angle errors. The version 1.2a of the Cornell 5GeV ERL lattice is used for this simulation. In the absence of sextupoles and other higher multipoles, we only analyze linear optics and analytical estimates for the effect of these three types of errors are presented. They are applied to the Cornell 5GeV ERL and compared to numerical simulations by *Tao* [1], according to which conclusions are drawn for the tolerance of the aforesaid errors. Adding sextupoles for chromoticity correction also introduces nonlinear dynamics into our system and a numerical analysis, as well as an analytical estimate, is done for the version 1.3a of the Cornell ERL lattice. In order to correct the particle orbit distortion incurred by various optical errors, two types of orbit feedback system, a local fast orbit feedback system on top of a global slow feedback system, are implemented in our system. We apply the singular value decomposition (SVD) algorithm in our simulation to adjust the steering strength of the dipole corrector magnets to minimize the rms orbit at the BPMs. In addition to the aforementioned optical errors, we also take into account the effect of random electronic noise in BPM signals and magnetic field errors caused by power supply fluctuations.

1 Introduction

In the Cornell 5GeV Energy Recovery Linac (ERL), the small beam size entailed by the goal of producing X-rays with high brilliance and coherence casts a tight constraint on the orbit error tolerance. Similiar requirements on the orbit stability are seen at other 3rd generation light sources. In Tab. 1, we list the orbit stability requirements and the stability achieved at different light sources [2, 3, 4, 5, 6, 7, 8, 10].

Extensive incremental improvements to orbit stabilization systems have been made at the Advanced Photon Source (APS) since it went in operation in 1996. The strategy for achieving true sub-micron orbit stability at the APS has been to study and compensate for multiple systematic effects and noise sources, enhance orbit correction feedback systems, and employ feedforward methodology where applicable [2]. At the European Synchrotron Radiation Facility (ESRF), in addition to a slow orbit correction (every 5 minutes), a fast global feedback system (4.4kHz) is implemented to correct, in the vertical direction, the fast orbit distortion caused by quadrupole magnet vibrations [4]. Similarly, a slow correction procedure is used at ELETTRA to counteract slow orbit motions and drifts due to thermal effects, while a number of local fast orbit feedback systems are installed to correct faster orbit disturbances generated by ID gap changes, by vibrations of the quadrupole magnets and by ripple of the magnet power supplies [6]. At the SPring-8, the sub-micron orbit stability is achieved not by the feedback systems alone but by the thorough source suppression as a first step and some proper feedback correction to push the stability up to sub-micron level as a

Table 1: Oribt Stability of Third-Generation Synchrotron Light Source

	Horizontal Orbit x [μm]		Vertical Oribt y [μm]	
	Requirement	Achieved	Requirement	Achieved
APS	14.0	12.6	0.45	0.59
ESRF	N/A	1.0	N/A	0.6
ALS	10.3	2	1.2	0.5
ELETTRA	5.0	0.85	5	0.47
SPring-8	28.0	4	0.4	1
SLS	N/A	1.0	0.7	0.6

second step [8]. In the Swiss Light Souce (SLS), long and short term orbit stability of the electron beam is achieved by dynamic alignment systems and by fast closed orbit feedback [9]. The SLS reproduces and stabilizes a previously established reference orbit within 1/10th of the vertical beam size corresponding to $\approx 1\mu$m at the insertion devices (IDs) [10, 11].

In our previous report [12], we discussed how the requirement for the power supply stability in the Cornell 5GeV ERL is estimated based upon the beam stability requirment in the ID sections. In our analysis, we mentioned that orbit tolerance can be relaxed if a global orbit feedback system is implemented for orbit correction. In this report, we will analyze in detail various sources of orbit errors and algorithms to correct them.

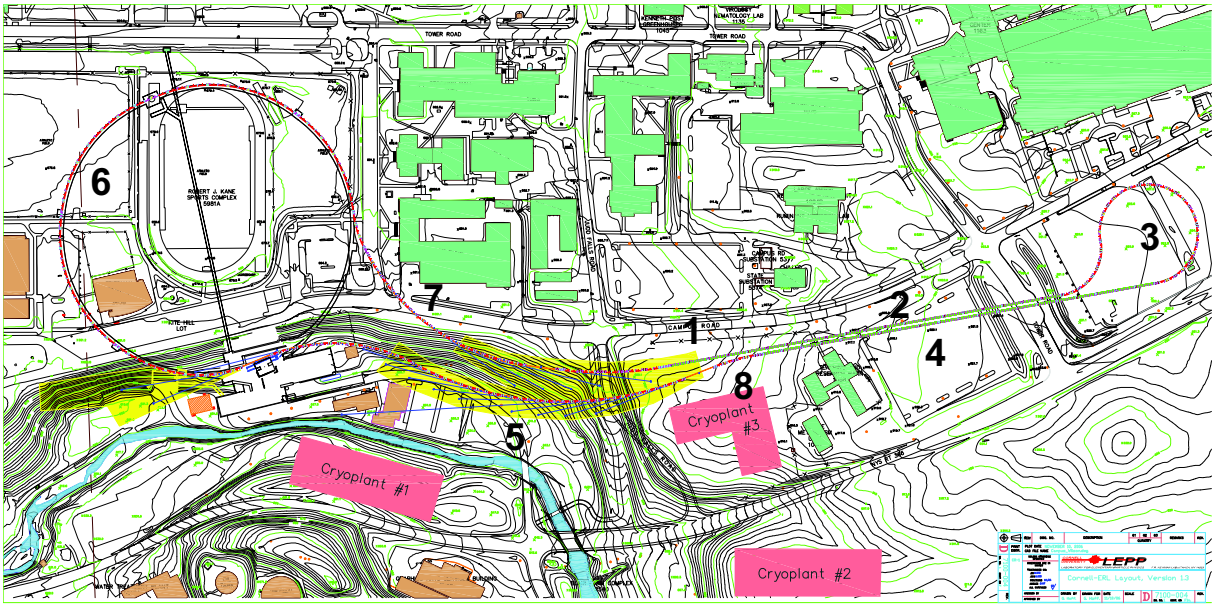

Figure 1: A Schematic Layout of Cornell 5GeV ERL

In the 1.2a version of the Cornell ERL lattice, a total number of 91 dipole magnets and 498 quadrupoles are installed in the two linacs, turn-around loop, south arc, north arc and return loop. Figure 1 is the schematic layout of the ERL planned at Cornell university [13]. The lines ② and ④ represent the linac part for accelerating and decelerating the beam. The smaller red circle ③ is the turn-around loop and the bigger red circle ⑥ is the return loop. The two red arcs ⑤ and ⑦ are the north and south arc where highly brilliant x-ray beams are generated. ⑧ is the injector and ① is the beam dump.

Several sources of orbit and optical errors are identified and simulated for this accelerator. Magnetic field errors caused by the power supply fluctuation can affect both the particle orbit and the optics in the ERL [12]. Magnetic field fluctuations can cause wrong beam steering effect leading to emittance growth and thus increase the beam size at the ID sections. Similarly Quadrupole field errors can affect the beta function and phase advance in both vertical and horizontal directions. Furthermore, a combination of the dipole field errors and the quadrupole field errors, albeit a second order effect, can have a significant impact on the particle's orbit in the insertion devices.

In addition to the power supply fluctuations, the misalignment of the accelerator components can lead to orbit distortions and beam emittance dilution. A misaligned quadrupole magnet can create, in addition to the quadrupole field for beam focusing, an effective dipole field that will introduce unwanted dispersion. An RF cavity with a pitch angle can accelerate the beam in off-axis directions, and thus produce time-varying transverse deflections that leads to emittance growth. Furthermore, wakefields created by the beam traversing misaligned RF cavities can also cause transverse deflections. Studies on the impact of these sources of errors has been done for the TESLA main linac [14]. It is concluded for the TESLA linac that, from the point of view of emittance preservation, the most crucial factor is the alignment of the quadrupoles to the beam axis, where 20μm rms offsets must be achieved. The tolerance for the RF pitch angles is about 100μrad (rms) and the beam-to-cavity offsets are far less crucial with 200μm rms offsets can be tolerated[14]. Such a conclusion is consistent with our simulation results, which show that the most stringent constraint is cast on the quadrupole misalignments. The typical magnitudes of the aforementioned magnetic and alignment errors and their effect on the particle orbit and beam emittance are listed in Tab. 2.

Orbit errors produced by the aforementioned sources can be effectively corrected by an orbit feedback system that comprises BPMs and beam steering magnets. These corrector magnets can steer the beam in a way that

Table 2: A summary of error sources and their effect on the beam (σ_x: rms beam size at the ID)

Dipole Magnetic Field Error (Correlated)	$\Delta B/B = 10^{-3}$	$\Delta x/\sigma_x = 0.7\%$
Dipole Magnetic Field Error (Uncorrelated)	$\sigma(\Delta B/B) = 2 \times 10^{-7}$	$\Delta x/\sigma_x \approx 20\%$
Quadrupole Magnetic Field Error (Uncorrelated)	$\sigma(\Delta k/k) = 10^{-3}$	$\Delta\sigma_x/\sigma_x = 10.6\%$
Combined Dipole and Quadrupole Errors	$\Delta B/B = 10^{-4}$, $\sigma(\Delta k/k) = 10^{-4}$	$\Delta x/\sigma_x = 5.4\%$
Quadrupole Misalignment	$\sigma(\Delta x) = \sigma(\Delta y) = 3 \times 10^{-4}$m	rms orbit$= 5 \times 10^{-2}$m
RF Cavity Pitch Angles	$\sigma(\Delta\theta) = 5 \times 10^{-4}$rad	$\Delta\varepsilon/\varepsilon \approx 0.1\%$

compensates the wrong steering from dipoles, quadrupoles and RF cavities. Generally speaking, there are two types of orbit feedback system based on different principles, which is demonstrated in Fig 2. In a slow orbit feedback system, the average bunch position of the train is measured and corrected for the next pulse. Such a system has a low sampling rate and is often used to correct slow varying perturbations. By contrast, a fast orbit feedback system measures the orbit offset of the first bunch and exerts a correction on the following bunch in the same pulse by a fast kicker [15].

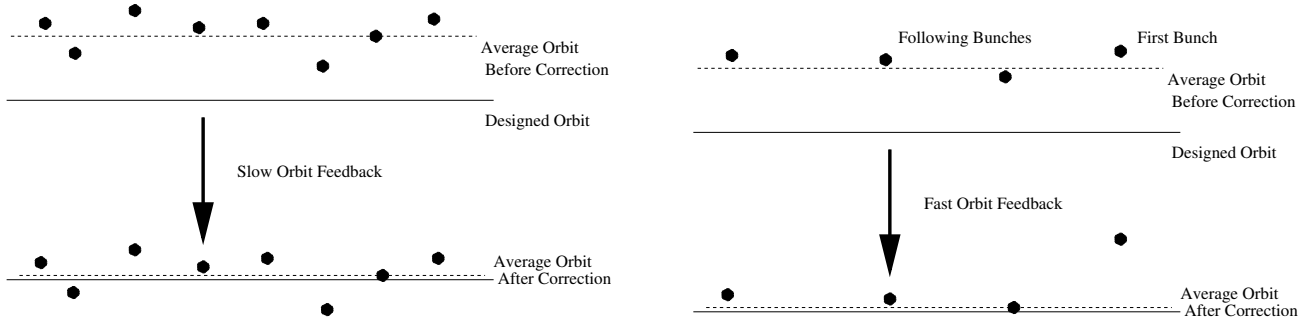

(a) A Slow Orbit Feedback System

(b) A Fast Orbit Feedback System

Figure 2: Schematic presentation of two different types of orbit feedback system

In the SLS, both a fast orbit feedback (FOFB) system and a slow orbit feedback (SOFB) system are implemented for compensating different types of orbit errors. The FOFB suppresses residual orbit oscillations up to 60Hz, while the SOFB on X-BPM readings can compensate for slow thermal drifts without interfering with the FOFB, by changing the FOBF reference resulting in sub-micron stability at the location of the X-BPM [10].

Similarly a system combining a slow global orbit feedback system with a fast local orbit feedback system at the IDs is simulated for the orbit correction in the Cornell ERL. It comprises beam position monitors (BPMs) and corrector magnets. The information of the particle's orbit is collected at each BPM and processed by computers. With the information about the orbit response matrix (ORM), the SVD algorithm is applied to find the proper magnetic strength of each corrector magnet, which minimizes the rms orbit at the BPMs. Similar to the global orbit feedback system adopted at SLS, which minimize the orbit variations at all experiments at the same time [16], the slow global orbit feedback system simulated for the Cornell ERL minimizes the rms orbit at every BPMs with equal weight. In contrast, the fast local feedback system weighs the BPMs in the IDs more heavily and thus stabilizes the orbit in the IDs with sub-micron precision. Similar to the requirement discussed in [10][11], the horizontal (vertical) orbit errors at the IDs are controled within 1/10th of the designed the horizontal (vertical) beam size ($\approx 3\mu$m) in those sections.

2 Sources of Orbit Errors in an ERL

2.1 Quadrupole Misalignments

In an accelerator with quadrupole magnets for beam focusing, the shift of a quadrupole's magnetic center from the center of the beam pipe can create an effective dipole magnetic field that will steer the beam.

The magnetic potential of a quadrupole magnet can be written as

$$\psi = \Psi_2 \Im\left\{(x - iy)^2\right\} = -2\Psi_2 xy\,, \tag{1}$$

where ψ_2 is multipole coefficient for a quadrupole magnetic field.

If the magnetic center of the quadrupole is shifted from the origin to $(\delta x, \delta y)$, its magnetic potential becomes

$$\psi = -2\Psi_2(x-\delta x)(y-\delta y) \approx -2\Psi_2 xy + \tilde{\Psi}_y x + \tilde{\Psi}_x y\,, \tag{2}$$

where an effective dipole magnetic field appears in both the horizontal and the vertical direction with $\tilde{\Psi}_x = 2\Psi_2\delta x$ and $\tilde{\Psi}_y = 2\Psi_2\delta y$. Thus the new magnetic field can be written as

$$\mathbf{B} = -\nabla\psi = (2\Psi_2 y - \tilde{\Psi}_y)\vec{e}_x + (2\Psi_2 x - \tilde{\Psi}_x)\vec{e}_y\,, \tag{3}$$

and the effective steering on the beam generated by such a misaligned quadrupole is

$$\begin{aligned}\Delta\theta_x &= -\frac{q}{P}\int_0^L \Delta B_y dz = \frac{q}{P}\tilde{\Psi}_x L = k_l\delta x\\ \Delta\theta_y &= \frac{q}{P}\int_0^L \Delta B_x dz = -\frac{q}{P}\tilde{\Psi}_y L = -k_l\delta y\,,\end{aligned} \tag{4}$$

where k_l is the integrated quadrupole strength and P is the particle's momentum.

Similar to our analysis in [12], we can calculate the horizontal and vertical orbit errors at ID sections as a result of the effective beam steering from misaligned quadrupoles. The horizontal and vertical orbit errors can be written as

$$\begin{aligned}\Delta x &= \sum_{n=1}^{N_q} r_x\xi_n k_{ln}\sqrt{\beta_x\beta_{xn}}\sqrt{\frac{P_n}{P}}\sin(\psi_x-\psi_{xn})\\ \Delta y &= -\sum_{n=1}^{N_q} r_y\zeta_n k_{ln}\sqrt{\beta_y\beta_{yn}}\sqrt{\frac{P_n}{P}}\sin(\psi_y-\psi_{yn})\,,\end{aligned} \tag{5}$$

where r_x and r_y are quadrupole alignment sensitivity factors, ξ_n and ζ_n are two Gaussian random variables, N_q is the total number of quadrupoles before an ID section, P_n and P are the designed particle's momenta in the n-th quadrupole and the ID section respectively, and β_x, β_y, ψ_x, ψ_y, β_{xn}, β_{yn}, ψ_{xn}, and ψ_{yn} are the respective Twiss parameters in the quadrupole and ID sections.

We are more concerned with the vertical and horizontal rms orbit errors in the ID sections, which can be calculated as

$$\begin{aligned}\langle\Delta x^2\rangle &= \sum_{n=1}^{N_q} r_x^2 k_{ln}^2\beta_x\beta_{xn}\frac{P_n}{P}\sin^2(\psi_x-\psi_{xn}) \le \left(\frac{\sigma_x}{10}\right)^2 = \frac{\beta_x\varepsilon_x}{100\gamma}\\ \langle\Delta y^2\rangle &= \sum_{n=1}^{N_q} r_y^2 k_{ln}^2\beta_y\beta_{yn}\frac{P_n}{P}\sin^2(\psi_y-\psi_{yn}) \le \left(\frac{\sigma_y}{10}\right)^2 = \frac{\beta_y\varepsilon_y}{100\gamma}\,,\end{aligned} \tag{6}$$

where $\langle\xi_n\xi_m\rangle = \delta_{mn}$ and $\langle\zeta_n\zeta_m\rangle = \delta_{mn}$ are applied. Similar to the requirement stated in [12], the rms orbit errors must be no larger than 1/10th of the designed horizontal beam size $\sigma_x = \beta_x\varepsilon_x/\gamma$ and vertical beam size $\sigma_x = \beta_y\varepsilon_y/\gamma$ in the IDs, where $\epsilon_x = \epsilon_y = 3\times10^{-7}$. Thus we can calculated the requirements for the alignment sensitivity factors as:

$$\begin{aligned}r_x &\le \frac{\sqrt{\varepsilon_x}}{10\sqrt{\gamma\sum_{n=1}^{N_q} k_{ln}^2\beta_{xn}\frac{P_n}{P}\sin^2(\psi_x-\psi_{xn})}}\\ r_y &\le \frac{\sqrt{\varepsilon_y}}{10\sqrt{\gamma\sum_{n=1}^{N_q} k_{ln}^2\beta_{yn}\frac{P_n}{P}\sin^2(\psi_y-\psi_{yn})}}\end{aligned} \tag{7}$$

According to Eq. (7), the alignment sensitivity requirement for the Cornell 5GeV ERL is about 3×10^{-8}m. Such a requirement is beyond the reach of current technology and thus an orbit feedback system must be implemented to insure the particle's orbit in the IDs is within the tolerance of our experiment.

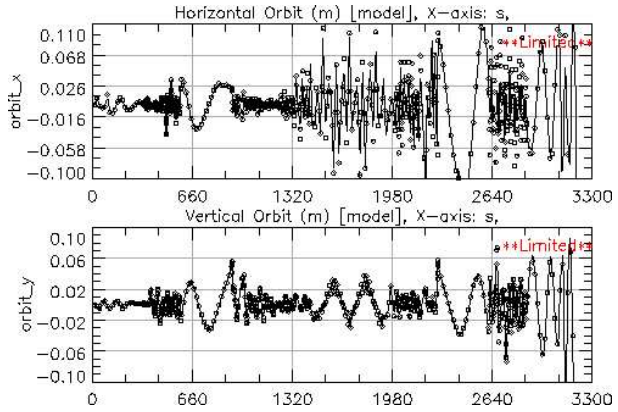

(a) Orbit error before correction

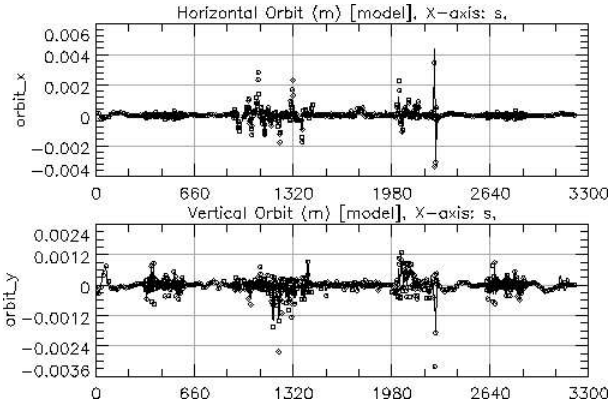

(b) Orbit error after correction

Figure 3: Orbit error caused by quadrupole misalignments and its correction

In an ERL the typical rms quadrupole misalignment is about 300μm and the rms orbit due to this misalignment without correction is about 50mm. The rms orbit can be reduced to about 500μm by using the SVD algorithm to find the appropriate strength of each individual steering magnet. Figure 3(a) shows the orbit before correction and Fig. 3(b) shows how the orbit is reduced after implementing a feedback system.

In addition to the beam steering effect, quadrupole misalignments can also cause variations of beta functions and betatron phase advances. This small focusing is not currently considered in other accelerators' design, but we estimate its effect for the Cornell ERL because of its sensitivity to beta function errors due to the small beam size. From Eq. (15) in [12], we can see that it's a second order effect. The effective κ_x and κ_y in a misaligned quadrupole can be written as:

$$\kappa_x = \frac{q}{P} B_{y0}\,, \qquad \kappa_y = -\frac{q}{P} B_{x0} \tag{8}$$

where the effective vertical and horizontal dipole fields B_{y0} and B_{x0} are given by

$$B_{y0} = -2\Psi_2 \Delta x\,, \qquad B_{x0} = -2\Psi_2 \Delta y \tag{9}$$

Thus we have

$$\kappa_x^2 = k^2 \Delta x^2\,, \qquad \kappa_y^2 = k^2 \Delta y^2 \tag{10}$$

According to Eq. (23) and Eq. (24) in [12], we can write the changes in beta function and betatron phase advance as:

$$\begin{aligned} \frac{\Delta\beta_x}{\beta_x} &= -k^2 \Delta x^2 L \beta_{x0} \sin 2\psi_x\,, \qquad \Delta\psi_x = k^2 \Delta x^2 L \beta_{x0} \sin^2 \psi_x \\ \frac{\Delta\beta_y}{\beta_y} &= -k^2 \Delta y^2 L \beta_{y0} \sin 2\psi_y\,, \qquad \Delta\psi_y = k^2 \Delta y^2 L \beta_{y0} \sin^2 \psi_y \end{aligned} \tag{11}$$

Thus the beta function error at the n-th element as a result of preceding quadrupole misalignments can be written as:

$$\begin{aligned} \frac{\Delta\beta_{xn}}{\beta_{xn}} &= -\sum_{m=1}^{N_q} k_m^2 \Delta x_m^2 L_m \beta_{xm} \sin 2(\psi_{xn} - \psi_{xm}) \\ \frac{\Delta\beta_{yn}}{\beta_{yn}} &= -\sum_{m=1}^{N_q} k_m^2 \Delta y_m^2 L_m \beta_{ym} \sin 2(\psi_{yn} - \psi_{ym}) \end{aligned} \tag{12}$$

If we write the random misalignments Δx_m and Δy_m as:

$$\Delta x_m = r_x \xi_m\,, \qquad \Delta y_m = r_y \zeta_m \tag{13}$$

where ξ and ζ are Gaussian random variables with $\langle \xi^2 \rangle = 1$ and $\langle \zeta^2 \rangle = 1$, we can calculate the average horizontal and vertical beam size changes.

$$\left\langle \frac{\Delta\sigma_{xn}}{\sigma_{xn}} \right\rangle = \frac{1}{2}\left\langle \frac{\Delta\beta_x}{\beta_x} \right\rangle = -\frac{1}{2}r_x^2 \sum_{m=1}^{N_q} (kL)_m^2 L_m \beta_{xm} \sin 2(\psi_{xn} - \psi_{xm})$$
$$\left\langle \frac{\Delta\sigma_{yn}}{\sigma_{yn}} \right\rangle = \frac{1}{2}\left\langle \frac{\Delta\beta_y}{\beta_y} \right\rangle = -\frac{1}{2}r_y^2 \sum_{m=1}^{N_q} (kL)_m^2 L_m \beta_{ym} \sin 2(\psi_{yn} - \psi_{ym}) \tag{14}$$

If the beam size variations are required to be less than 1/10th of the designed value, we have

$$r_x \leq \frac{\sqrt{0.2}}{\sqrt{\sum_{m=1}^{N_q} (kL)_m^2 L_m \beta_{xm} |\sin 2(\psi_{xn} - \psi_{xm})|}}$$
$$r_y \leq \frac{\sqrt{0.2}}{\sqrt{\sum_{m=1}^{N_q} (kL)_m^2 L_m \beta_{ym} |\sin 2(\psi_{yn} - \psi_{ym})|}} \tag{15}$$

According to Eq. (14), the sensitivity requirement from the beam size tolerance in the IDs is about 5×10^{-2}m. Compared to the sensitivity requirement from Eq. (7), this one is less critical. Figure 4 shows how 300μm rms quadrupole misalignment changes the beta function in the Cornell ERL lattice and its correction by the same global orbit feedback system employed for the orbit correction.

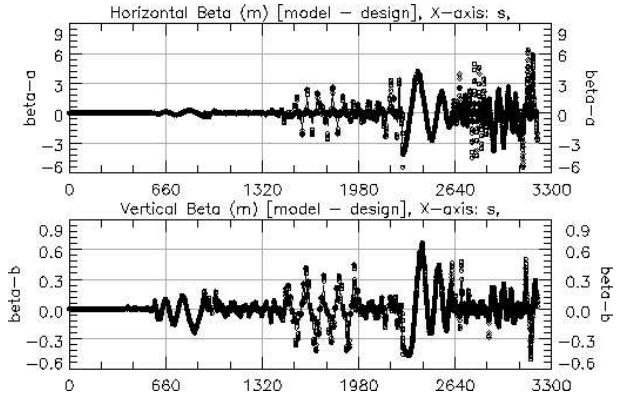

(a) Beta function error before correction

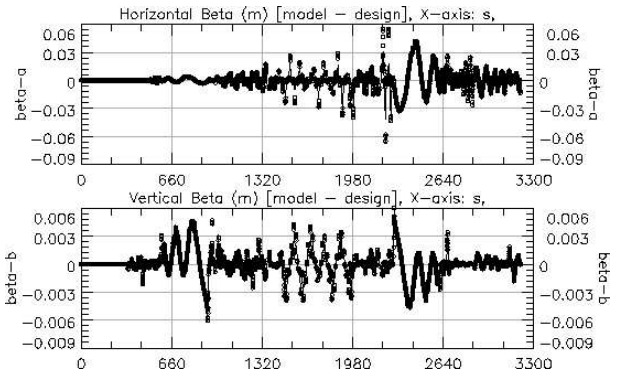

(b) Beta function error after correction

Figure 4: Beta function error caused by quadrupole misalignments and its correction

2.2 Dipole Field Errors

An error of the dipole magnetic field can cause the bend to steer the beam differently from its designed trajectory. In our previous report [12], we have already analyzed how Gaussian random dipole field errors affect the particle orbits in the IDs. The rms orbit error at a ID section is:

$$\langle \Delta x^2 \rangle = \sum_{n=1}^{N_d} r_\theta^2 \theta_n^2 \frac{P_n}{P} \beta_{xn} \beta_x \sin^2(\psi_x - \psi_{xn}) \tag{16}$$

where r_θ represents the rms relative field error, θ_n is the bending angle of the n-th dipole, P_n and P are the particle's momenta in the dipole and ID section respectively, and β_{xn}, β_x, ψ_x and ψ_{xn} are Twiss parameters.

As stated in [12], the orbit error is required to be less than 1/10th of the designed beam size at the IDs, which gives:

$$\langle \Delta x^2 \rangle = \sum_{n=1}^{N_d} r_\theta^2 \theta_n^2 \frac{P_n}{P} \beta_{xn} \beta_x \sin^2(\psi_x - \psi_{xn}) \leq \left(\frac{\sigma_x}{10}\right)^2 = \frac{\beta_x \varepsilon_x}{100\gamma}$$

$$r_\theta \leq \frac{\sqrt{\varepsilon_x}}{10\sqrt{\gamma \sum_{n=1}^{N_d} \theta_n^2 \frac{P_n}{P} \beta_{xn} \sin^2(\psi_x - \psi_{xn})}} \tag{17}$$

An estimate of the required dipole field error sensitivity is made in [12] and without a feedback system, a sensitivity of about 2×10^{-7} is required for the Cornell 5GeV ERL. Current technology can provide a dipole field that is stable at a level of 10^{-5} and the rms orbit due to such field fluctuation is about 100μm. It can be reduced to about 1μm by steering magnets. Figure 5 shows how Gaussian random magnetic field errors can generate horizontal orbit errors along the accelerator and how they can be corrected by a feedback system.

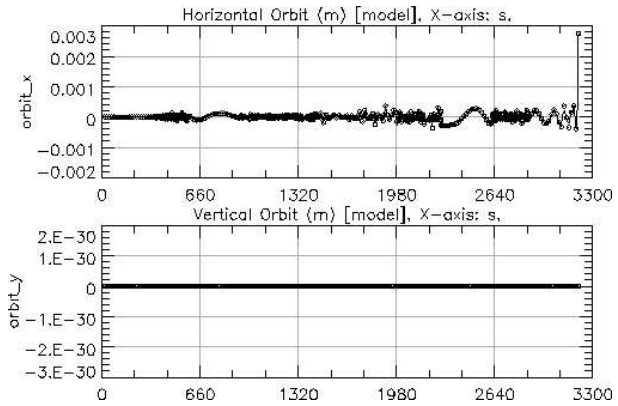

(a) Orbit error before correction

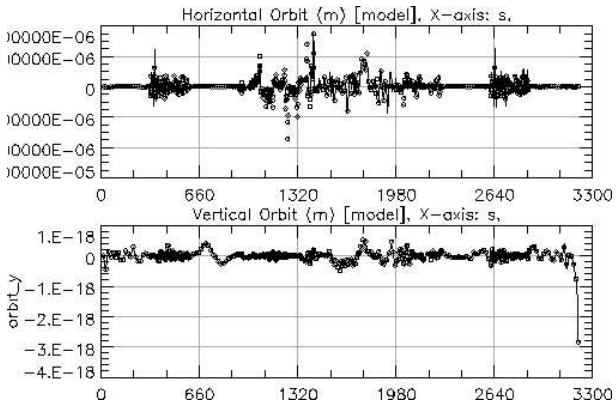

(b) Orbit error after correction

Figure 5: Orbit error caused by dipole magnetic field errors and its correction

2.3 RF Cavity Pitch Angles

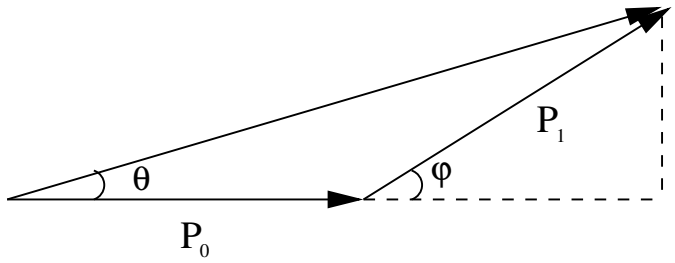

Figure 6: Beam steering by an RF cavity with a pitch angle φ

If the RF cavity has a pitch angle φ, the beam can gain off-axis momentum while traversing such a cavity and the effective steering can be written as

$$\Delta\theta \approx \tan\Delta\theta = \frac{P_1 \sin\varphi}{P_0 + P_1 \cos\varphi} \approx \frac{\Delta P}{P}\varphi \tag{18}$$

Table 3: A summary of different sources of orbit error and their correction

	Quad Misalignments ($\sigma = 0.3$mm)		Dipole Errors ($\sigma = 10^{-5}$)		RF Cavity Pitch Angles ($\sigma = 0.5$mrad)	
	Before [mm]	Corrected [μm]	Before [mm]	Corrected [μm]	Before [mm]	Corrected [μm]
x	47	440	0.14	1.0	0.59	52
y	36	350	0	0	0.47	41

where P_0 is the initial on-axis momentum, P is the final on-axis momentum and $P_1 = \Delta P$ is the momentum gain from the RF cavity.

Similar to the orbit error caused by dipole field errors, the horizontal and vertical rms orbit errors at the IDs as a result of RF cavity pitch angles can be written as

$$\begin{aligned}\langle \Delta x^2 \rangle &= \sum_{n=1}^{N_c} \varphi_x^2 \frac{\Delta P_n^2}{P_n P} \beta_x \beta_{xn} \sin^2(\psi_x - \psi_{xn}) \\ \langle \Delta y^2 \rangle &= \sum_{n=1}^{N_c} \varphi_y^2 \frac{\Delta P_n^2}{P_n P} \beta_y \beta_{yn} \sin^2(\psi_y - \psi_{yn})\end{aligned} \tag{19}$$

where φ_x and φ_y are horizontal and vertical rms pitch angles. The requirement for the orbit errors in ID sections give us:

$$\begin{aligned}\varphi_x &\leq \frac{\sqrt{\varepsilon_x}}{10\sqrt{\gamma \sum_{n=1}^{N_c} \frac{\Delta P_n^2}{P_n P} \beta_{xn} \sin^2(\psi_x - \psi_{xn})}} \\ \varphi_y &\leq \frac{\sqrt{\varepsilon_y}}{10\sqrt{\gamma \sum_{n=1}^{N_c} \frac{\Delta P_n^2}{P_n P} \beta_{yn} \sin^2(\psi_y - \psi_{yn})}}\end{aligned} \tag{20}$$

According to Eq. (20), the rf pitch angle can be no larger than 1μrad in the Cornell 5GeV ERL. In today's accelerators the typical rms RF cavity pitch angle is about 500μrad and the rms orbit due to such angles is about 1mm. Thus a feedback system must be implemented to compensate the steering effect from pitched rf cavities. Figure 7 shows how orbit errors as a result of pitched rf cavities are corrected in the 1.2a version of the Cornell ERL lattice.

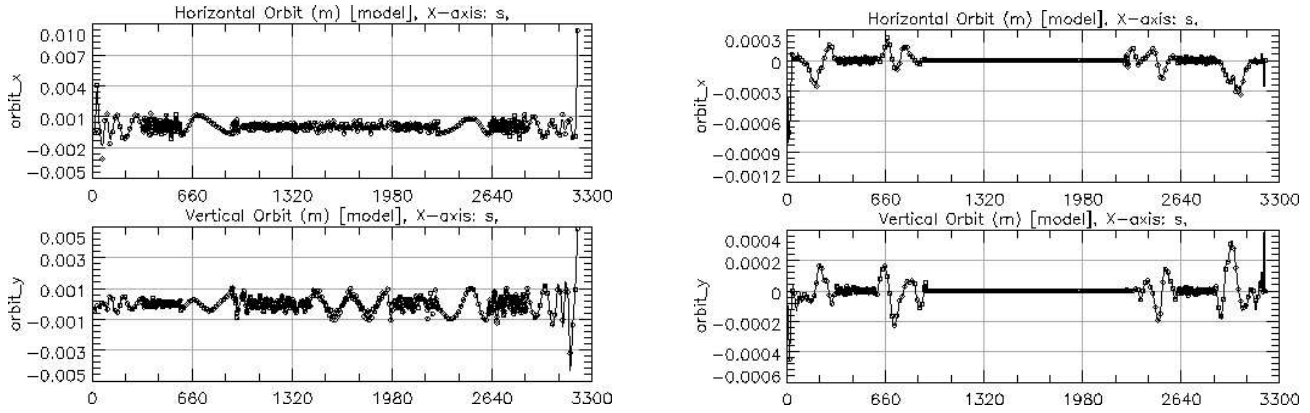

(a) Orbit error before correction

(b) Orbit error after correction

Figure 7: Orbit error caused by RF cavity pitch angles and its correction

The various sources of orbit errors and the results of their correction by orbit feedback systems are listed in Tab. 3. The distribution of random errors is assumed to be Gaussian with 3σ cutoff.

In addition to causing particle orbit errors, a pitched cavity can generate emittance growth as well. Similar to the emittance dilution due to transverse coupler kicks [18], a pitched RF cavity has time-varying transverse electric field that can deflect the beam. The transverse deflecting force can be written as:

$$\Delta F_\perp = eE \sin\theta_p \cos(\omega_{RF}\Delta t + \psi_0) \tag{21}$$

where E is the field gradient, θ_p is the cavity's pitch angle, ω_{RF} is the frequency of the accelerating mode, Δt is the time delay for a off-center particle and ψ_0 is the RF phase corresponding to the center of the bunch.

The total transverse momentum change for a particle traversing the cavity is :

$$\Delta P_\perp = \Delta F_\perp \cdot T \tag{22}$$

where $T = L_{RF}/c$ is the traveling time for an ultra-relativistic particle. The final result for the transverse momentum change can be written as:

$$\Delta P_\perp \approx \frac{e}{c} E L_{RF} \sin\theta_p [\cos\psi_0 - \omega_{RF}\Delta t \sin\psi_0] \tag{23}$$

Here the formula is linearized in Δt.

If we assume that all RF cavities are pitched in y direction, the change in y' for a particle with nominal momentum P is:

$$\Delta y' = \frac{\Delta P_y}{P} \approx \frac{eEL_{RF}}{Pc} \sin\theta_p \left[\cos\psi_0 - \omega_{RF}\Delta t \sin\psi_0\right] \tag{24}$$

where the first term does not vary with Δt and thus has no contribution to the emittance dilution. The second term varies for different particles in the same bunch with different Δt, which causes the emittance growth.

Similar to what is done in [18], we begin with a Gaussian beam distribution defined by

$$\rho_0(y, y', \Delta t) = \frac{1}{2\pi\varepsilon_{y0}} e^{-\frac{\gamma y^2 + 2\alpha y y' + \beta y'^2}{2\varepsilon_{y0}}} \frac{1}{\sqrt{2\pi}\sigma_t} e^{-\frac{\Delta t^2}{2\sigma_t^2}} \tag{25}$$

where β, α and γ are twiss parameters, ε_0 is the designed vertical emittance and σ_t is the bunch length.

Ignoring the constant term in Eq. (24), we can add the change in y' into Eq. (25)

$$\rho(y, y', \Delta t) = \frac{1}{2\pi\varepsilon_{y0}} e^{-\frac{\gamma y^2 + 2\alpha y (y' - S\Delta t) + \beta (y' - S\Delta t)^2}{2\varepsilon_{y0}}} \frac{1}{\sqrt{2\pi}\sigma_t} e^{-\frac{\Delta t^2}{2\sigma_t^2}} \tag{26}$$

where $S = \dfrac{\omega_{RF}}{c} L_{RF} \dfrac{eE}{P} \sin\theta_p \sin\psi_0$. The final emittance is the average of the Courant-Schnyder invariant over the beam distribution

$$\varepsilon_y = \int \frac{1}{2}(\gamma y^2 + 2\alpha y y' + \beta y'^2)\rho(y, y', \Delta t) dy dy' d\Delta t \tag{27}$$

which is evaluated in [18] to give the result

$$\varepsilon_y = \varepsilon_{y0} + \frac{1}{2}\beta S^2 \sigma_t^2 \tag{28}$$

Thus the total emittance growth due to the RF pitch angles is given by

$$\Delta\varepsilon_y = \sum_{n=1}^{N_{RF}} \frac{1}{2}\beta_n S_n^2 \sigma_t^2 \,, \qquad S_n = \frac{\omega_{RF}}{c} L_n \frac{eE_n}{P_n} \sin(\xi_n\theta_p) \sin\psi_0 \tag{29}$$

where N_{RF} is the total number of accelerating RF cavities, ξ_n is a Gaussian random variable with $\langle \xi_n^2 \rangle = 1$ and σ_{θ_p} is the rms RF cavity pitch angle.

According to Eq. 29, the tolerance on the emittance growth of our ERL operation dictates the tolerance of the RF cavity pitch angle. The average emittance growth can be written as

$$\langle \Delta\varepsilon_y \rangle = \frac{1}{2} \sum_{n=1}^{N_{RF}} \beta_n \left(\frac{\omega_{RF}}{c} L_n \frac{eE_n}{P_n} \sin\psi_0 \right)^2 \sigma_t^2 \langle \sin^2(\xi_n \sigma_{\theta_p}) \rangle \tag{30}$$

Table 4: Cornell ERL Parameter List

Parameters	ω_{RF}[GHz]	L_{RF}[m]	E[MV/m]	ψ_0 [degree]	σ_{θ_p}[mrad]	ε_{y0}[mm·mrad]	σ_t [fs]
High Flux Mode	1.3	0.84	16	9	1.5	0.3	2000

Assuming $\xi_n\theta_p \ll 1$ we have

$$\langle \Delta\varepsilon_y \rangle = \frac{1}{2}\sigma_{\theta_p}^2 \sum_{n=1}^{N_{RF}} \beta_n \left(\frac{\omega_{RF}}{c} L_n \frac{eE_n}{P_n} \sin\psi_0 \right)^2 \sigma_t^2 \langle \xi_n^2 \rangle \tag{31}$$

Thus the rms RF pitch angle θ_p must satisfy

$$\sigma_{\theta_p} \leq \sqrt{\frac{2\Delta\varepsilon_{\text{tolerance}}}{\sum_{n=1}^{N_{RF}} \beta_n \left(\frac{\omega_{RF}}{c} L_n \frac{eE_n}{P_n} \sin\psi_0 \right)^2 \sigma_t^2}} \tag{32}$$

For the Cornell ERL, the typical values of the parameters are listed in Tab. 4. With these parameters, we can calculate the tolerance of the rf pitch angle for an emittance growth less than 10%. The result is $\sigma_{\theta_p} \leq 1.5$mrad. We can also simulate how the normalized emittance grows as the beam being accelerated along the linac. Figure 8 shows the emittance growth as a result of a Gaussian random distribution of the RF pitch angles with parameters specified in Tab. 4. This is for a particular random seed and different choices of the seed give similar results.

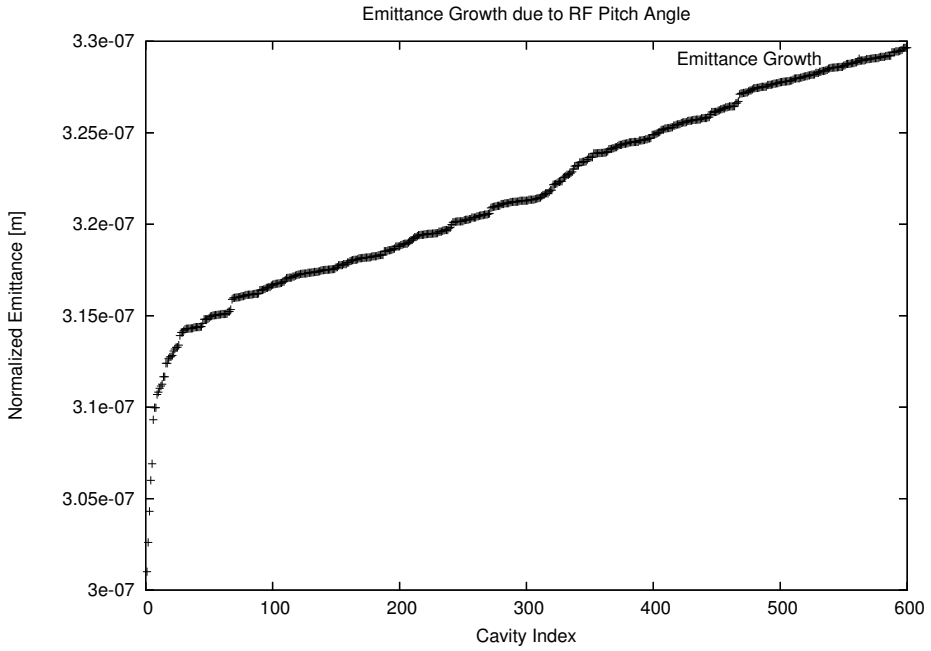

Figure 8: The emittance growth along the linac with randomly pitched cavities

For bunches that are on crest ($\psi_0 = 0$), Eq. 24 becomes

$$\Delta y' \approx \frac{eEL_{RF}}{Pc} \sin\theta_p [1 - \frac{1}{2}(\omega_{RF}\Delta t)^2] \tag{33}$$

Similarly, we ignore the constant term and add the change in y' into Eq. 25:

$$\rho(y, y' - \tilde{S}\Delta t^2, \Delta t) = \frac{1}{2\pi\varepsilon_{y0}} e^{-\frac{\gamma y^2 + 2\alpha y(y' - S\Delta t^2) + \beta(y' - \tilde{S}\Delta t^2)^2}{2\varepsilon_{y0}}} \frac{1}{\sqrt{2\pi}\sigma_t} e^{-\frac{\Delta t^2}{2\sigma_t^2}} \tag{34}$$

where $\tilde{S} = \frac{\omega_{RF}^2}{2c} L_{RF} \frac{eE}{P} \sin\theta_p$ and the final emittance can be calculated as

$$\begin{aligned}
\varepsilon_y &= \int \frac{1}{2}(\gamma y^2 + 2\alpha y y' + \beta y'^2)\rho(y, y' - \tilde{S}\Delta t^2, \Delta t) dy dy' d\Delta t \\
&= \int \frac{1}{2}\{\gamma y^2 + 2\alpha y(y' + \tilde{S}\Delta t^2) + \beta(y' + \tilde{S}\Delta t^2)^2\}\rho(y, y' - S\Delta t^2, \Delta t) dy dy' d\Delta t \\
&= \varepsilon_{y0} + \frac{3}{2}\beta \tilde{S}^2 \sigma_t^4
\end{aligned} \tag{35}$$

Thus we can see that the emittance growth become a second order effect. Similar to the case of off-crest bunches, we can calculate the tolerance of the RF pitch angle for the on-crest case and the result is given by

$$\sigma_{\theta_p} \leq \sqrt{\frac{2\Delta\varepsilon_{\text{tolerance}}}{3\sum_{n=1}^{N_{RF}} \beta_n \left(\frac{\omega_{RF}^2}{2c} L_n \frac{eE_n}{P_n}\right)^2 \sigma_t^4}} \tag{36}$$

The estimate for σ_{θ_p} with parameters listed in Tab. 4 is about 4.6 mrad. Figure 9 shows how the normalized emittance grows along the linac for on-crest bunches.

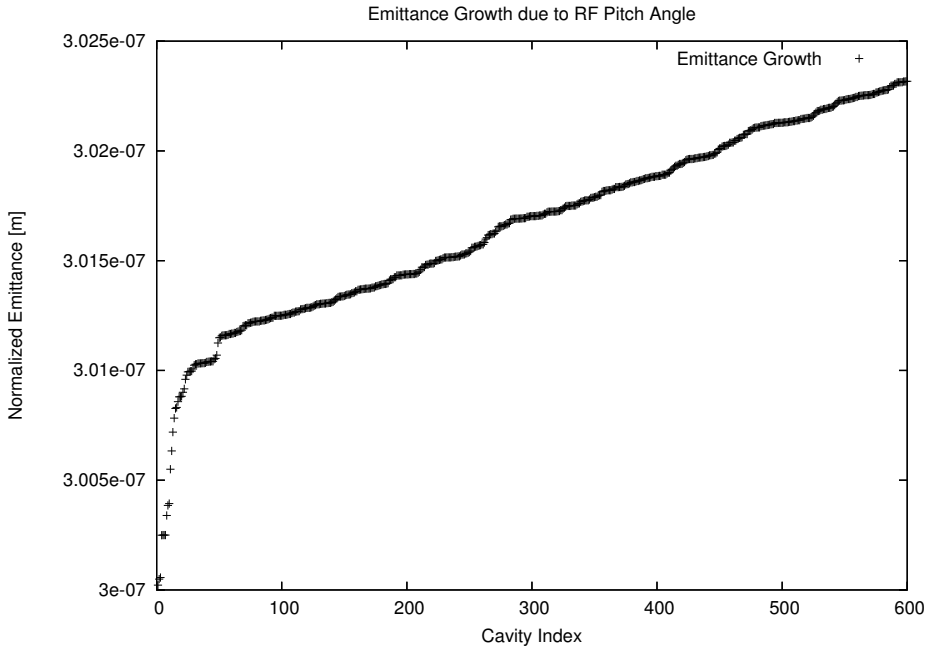

Figure 9: The emittance growth along the linac with randomly pitched cavities

3 Orbit Correction in an ERL

3.1 A General Theory of Orbit Correction in a Linear Lattice

For a linear system, we have already derived the orbit response at a particular element due to dipole steerings in [12]. Generally if multiple steering magnets are placed before one beam position monitor, the reading of this BPM is

$$x_i = x_{i0} + \sum_j \sqrt{\frac{P_j}{P_i}} \sqrt{\beta_i \beta_j} \sin(\psi_i - \psi_j) \Delta\vartheta_j \tag{37}$$

If we install m BPMs in the accelerator and n beam steering magnets, the readings at different BPMs can be related to the kick exerted by those magnets in a simple way:

$$\begin{pmatrix} x_1 \\ x_2 \\ \vdots \\ x_{m-1} \\ x_m \end{pmatrix} = \begin{pmatrix} x_{01} \\ x_{02} \\ \vdots \\ x_{0m-1} \\ x_{0m} \end{pmatrix} + \mathbf{O}_{m\times n} \begin{pmatrix} \Delta\vartheta_1 \\ \Delta\vartheta_2 \\ \vdots \\ \Delta\vartheta_{n-1} \\ \Delta\vartheta_n \end{pmatrix} \tag{38}$$

where $\mathbf{O}_{m\times n}$ is the orbit response matrix and its element O_{ij} can be calculated as

$$O_{ij} = \sqrt{\frac{P_j}{P_i}}\sqrt{\beta_i\beta_j}\sin(\psi_i - \psi_j)\,, \quad \psi_i > \psi_j \tag{39}$$

where elements with $\psi_i < \psi_j$ must be zero in a linear lattice because one steering magnet can only affect BPMs after itself.

It is often convenient to use the magnetic field strength instead of the kicking strength in an ERL problem, because kicks from steering magnets depend on the beam energy. Thus we can redefine the orbit response matrix as

$$O_{ij} = \frac{q}{P_j}\sqrt{\frac{P_j}{P_i}}\sqrt{\beta_i\beta_j}\sin(\psi_i - \psi_j)\,, \quad \psi_i > \psi_j \tag{40}$$

and Eq. (38) can be rewritten as

$$\begin{pmatrix} x_1 \\ x_2 \\ \vdots \\ x_{m-1} \\ x_m \end{pmatrix} = \begin{pmatrix} x_{01} \\ x_{02} \\ \vdots \\ x_{0m-1} \\ x_{0m} \end{pmatrix} + \mathbf{O}_{m\times n} \begin{pmatrix} B_1 \\ B_2 \\ \vdots \\ B_{n-1} \\ B_n \end{pmatrix} \tag{41}$$

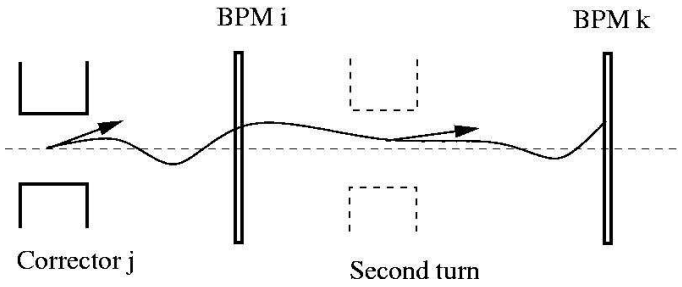

Figure 10: Beam steering in an ERL

One exception should be made for an ERL because the beam goes through part of the accelerator two times and is affected by some of the steering magnets twice during different turns. In such a case, the beam's energy needs to be taken into account when the matrix element is calculated. In a dipole magnet, we have the 0^{th} order equation of motion:

$$x' = \kappa_x = \frac{q}{P_0}B_{y0} \tag{42}$$

Thus if the kicks from one magnet in the first turn and the second turn are

$$\Delta\vartheta_1 = \frac{q}{P_1}B_{y0} \qquad \Delta\vartheta_2 = \frac{q}{P_2}B_{y0} = \frac{P_{01}}{P_{02}}\Delta\vartheta_1 \tag{43}$$

Thus if we use the magnetic strength as the variable and the steering magnet has indices j in the first turn and $j+N$ in second turn, where N is the total number of elements in the whole lattice. The matrix element in the orbit response matrix can be written as

$$O_{ij} = q\left[\sqrt{\frac{\beta_i\beta_j}{P_iP_j}}\sin(\psi_i - \psi_j) + \sqrt{\frac{\beta_i\beta_{j+N}}{P_iP_{j+N}}}\sin(\psi_i - \psi_{j+N})\right] \tag{44}$$

Our goal is correcting the particle orbit at those BPMs in the least square sense. Assume after corrections are applied at those steering magnets, particle's new orbit becomes

$$\vec{s} = \vec{x}_{\rm old} + \mathbf{O}\Delta\vec{\vartheta} \tag{45}$$

The quantity we want to minimize is

$$|\vec{s}|^2 = \vec{s}^{\rm T}\vec{s} \tag{46}$$

This quantity can be written in terms of the magnetic strength at each magnets and the orbit response matrix:

$$|\vec{s}|^2 = |\vec{x}_{\rm old}|^2 + \vec{x}_{\rm old}^{\rm T}\mathbf{O}\Delta\vec{\vartheta} + \Delta\vec{\vartheta}^{\rm T}\mathbf{O}^{\rm T}\vec{x}_{\rm old} + \Delta\vec{\vartheta}^{\rm T}\mathbf{O}^{\rm T}\mathbf{O}\Delta\vec{\vartheta} \tag{47}$$

At the minimal we have

$$\frac{\partial|\vec{s}|^2}{\partial\Delta\vartheta_i} = 0 \tag{48}$$

$$(\vec{x}_{\rm old}^{\rm T}\mathbf{O})_i + (\mathbf{O}^{\rm T}\vec{x}_{\rm old})_i + 2\sum_{j=1}^{n}(\mathbf{O}^{\rm T}\mathbf{O})_{ij}\Delta\vartheta_j = 0$$

Combining equations for different $\Delta\vartheta$, we have one vector equation

$$\mathbf{O}^{\rm T}\vec{x}_{\rm old} + \mathbf{O}^{\rm T}\mathbf{O}\Delta\vec{\vartheta} = 0 \tag{49}$$

and the solution for our magnetic strength is

$$\Delta\vec{\vartheta} = -(\mathbf{O}^{\rm T}\mathbf{O})^{-1}\mathbf{O}^{\rm T}\vec{x}_{\rm old} \tag{50}$$

From Eq. (50) we can see that if we have equal numbers of BPMs and steering magnets, the magnetic strength becomes

$$\Delta\vec{\vartheta} = -\mathbf{O}^{-1}\vec{x}_{\rm old} \tag{51}$$

and the particle's orbit at each BPM can be completely corrected as $\vec{x}_{\rm new} = 0$.

3.2 Orbit Correction by Singular Value Decomposition(SVD) algorithm

The orbit response matrix $\mathbf{O}$ is often singular or very close to singular in a real accelerator. In this case SVD algorithm produces a solution that is the best approximation for an overdetermined system in the least-square sense.

SVD methods are based on the following theorem of linear algebra: any $M \times N$ matrix $\mathbf{A}$ whose number of rows M is greater than or equal to its number of columns N, can be written as the product of an $M \times N$ column-orthogonal matrix $\mathbf{U}$, and $N \times N$ diagonal matrix $\mathbf{W}$ with positive or zero elements(the singular values), and the transpose of an $N \times N$ orthogonal matrix $\mathbf{V}$.

$$\mathbf{A} = \mathbf{U}\mathbf{W}\mathbf{V}^T \tag{52}$$

where

$$\mathbf{U}^T\mathbf{U} = \mathbf{V}^T\mathbf{V} = \mathbf{I} \tag{53}$$

For an overdetermined linear system described by the equation

$$\mathbf{A}\vec{x} = \vec{b} \tag{54}$$

the solution that minimizes the quantity $r \equiv |\mathbf{A}\vec{x} - \vec{b}|^2$ is obtained by calculating the pseudo-inverse of matrix $\mathbf{A}$.

$$\vec{x} = \mathbf{V} \cdot [\mathrm{diag}(1/w_j)] \cdot \mathbf{U}^T \cdot \vec{b} \tag{55}$$

Those singular values of w_j are replaced by 0 in $\mathrm{diag}(1/w_j)$.

Thus in the orbit correction scheme we can calculate the corresponding $\mathbf{U}$, $\mathbf{W}$ and $\mathbf{V}$ of the orbit response matrix and the magnetic field strength of the corrector magnets is determined by

$$\Delta\vec{\theta} = -\mathbf{V} \cdot [\mathrm{diag}(1/w_j)] \cdot \mathbf{U}^T \cdot \vec{x}_{\rm old} \tag{56}$$

It can be shown that this solution is equivalent to the solution we get from setting the first derivative to be zero in cases that have no singular value involved.

$$\begin{aligned}\Delta\vec{\theta} &= -(\mathbf{O}^{\rm T}\mathbf{O})^{-1}\mathbf{O}^{\rm T}\vec{x}_{\rm old} = -(\mathbf{V}\mathbf{W}\mathbf{U}^{\rm T}\mathbf{U}\mathbf{W}\mathbf{V}^{\rm T})^{-1}\mathbf{V}\mathbf{W}\mathbf{U}^{\rm T}\vec{x}_{\rm old} = -\mathbf{V}\mathbf{W}^{-2}\mathbf{V}^{\rm T}\mathbf{V}\mathbf{W}\mathbf{U}^{\rm T}\vec{x}_{\rm old} \\ &= -\mathbf{V} \cdot [\mathrm{diag}(1/w_j)] \cdot \mathbf{U}^{\rm T} \cdot \vec{x}_{\rm old}\end{aligned} \tag{57}$$

3.3 Simulation Results of the Orbit Correction in an ERL

In an ERL, one particle travels through the linac part of the accelerator two times, one for acceleration and the other for deceleration. Because the particle has different energies on its first and second turn, the kick it experiences from the same steering magnet is different. One BPM reads both the orbit of the high energy particles and the low energy partilcs and one steering magnet kick the particles according to their energy. In this case, the number of the beam's position measured by BPMs is always greater than the number of the steering magnets that can be manipulated in order to minimize the orbit error. Thus a complete orbit correction is impossible in an ERL by applying steering magnets alone.

Although the orbit can be corrected in a least square sense, we still need to evaluate the effectiveness of the orbit correction because small errors at the BPMs does not guarantee small errors everywhere. In effect, bad positioning of BPMs can cause the particle orbit diverge at certain locations in the accelerator. In the simulation we can put BPMs at every element in the lattice and compare this result with the result of putting BPMs at certain locations. This comparison could help us determine where the BPMs should be installed.

In the simulation we misalign all quadrupoles according to a Gaussian distribution with $\sigma = 0.1$mm and 3σ cutoff. The resulting orbit distortion is about 10mm and can be corrected by an orbit correction program using SVD algorithm. The average improvement of the horizontal orbit is about a factor of 55 (0.2mm) and the vertical orbit is improved by about a factor of 44 (0.2mm) (Average over 60 random seeds).

References

[1] J. Smith, D. Sagan, *The Tao Manual* (Draft)

[2] O. Singh, G. Decker, *Beam Stability at the Advanced Photon Source*, PAC'05, Knoxville, 2005

[3] G. Decker, O. Singh, *Orbit Feedback Using X-Ray Beam Position Monitoring at the Advanced Photon Source*, Invited talk WECI001 at ICALEPCS'01, San Jose, 2001

[4] L. Zhang, L. Farvacque, et al., *Electron Beam Stabilization Experiences at the ESRF*, Advanced ICFA Beam Dynamics Workshop on Nanometre-Size Colliding Beams, Lausanne, 2002

[5] C. Steier, *Stability Issues at the ALS*, NLSL-II Workshop, BNL, 2007

[6] D. Bulfone, R. De Monte, et al., *Status of the ELETTRA Global Orbit Feedback Project*, EPAC'06, Edinburgh, 2006

[7] D. Bulfone, R. De Monte, et al., *Design of a Fast Global Orbit Feedback System for the ELETTRA Storage Ring*, ICALEPCS'05, Geneva, 2005

[8] H. Tanaka, H. Aoyagi, et al, *Beam Orbit Stabilization at the SPring-8 Storage Ring*, Proceedings of the 7th International Workshop on Accelerator Alignment, SPring-8, 2002

[9] A. Streun, M. Böge, et al., *Beam Stability and Dynamic Alignment at SLS*, SSILS'01, Shanghai, 2001.

[10] M. Böge, B. Keil, et al., *Orbit Stability at the SLS*, PSI Scientific Report 2003, Vol. VI

[11] T. Schilcher, M. Böge, M. Dehler, et al., *Global Orbit Feedback System for the SLS Storage Ring*, ICALEPCS'99, Trieste, 1999

[12] C. Song, G.H. Hoffstaetter, *Magnetic Field Error Sensitivity in an Energy Recovery Linac*, Report Cornell-ERL-07-03 (2007)

[13] G.H. Hoffstaetter, I.V. Bazarov, etc. *Status of a Plan for an ERL Extension to CESR*, Proceedings PAC'05, Knoxville/TN (2005)

[14] P. Tenenbaum, R. Brinkmann, V. Tsakanov, *Beam-Based Alignment of the TESLA Main Linac*, EPAC'02, Paris, 1999

[15] R. Wanzenberg, *Review of Beam Dynamics and Instabilities in Linear Colliders*, LINAC'96, Geneva, 1996

[16] M. Böge, M. Dehler, et al. *Fast Closed Orbit Control in the SLS Storage Ring*, PAC'99, New York, 1999

[17] T.O. Raubenheimer, *Estimates of Emittance Dilution and Stability in High-energy Linear Accelerators*, PRST-AB, Vol.3, 121002 (2002)

[18] B. Buckley, G.H. Hoffstaetter, *Emittance Dilution due to Transverse Coupler Kicks in the Cornell ERL*,